Properties of ivabradine-induced block of HCN1 and HCN4 pacemaker channels

A. Bucchi, A. Tognati, R. Milanesi, M. Baruscotti and D. DiFrancesco

Laboratory of Molecular Physiology and Neurobiology, Department of Biomolecular Sciences and Biotechnology, University of Milano, via Celoria 26, 20133 Milan, Italy

Ivabradine is a 'heart rate-reducing' agent able to slow heart rate, without complicating side-effects. Its action results from a selective and specific block of pacemaker f-channels of the cardiac sinoatrial node (SAN). Investigation has shown that block by ivabradine requires open f-channels, is use dependent, and is affected by the direction of current flow. The constitutive elements of native pacemaker channels are the hyperpolarization-activated cyclic nucleotide-gated (HCN) channels, of which four isoforms (HCN1–4) are known; in rabbit SAN tissue HCN4 is expressed strongly, and HCN1 weakly. In this study we have investigated the blocking action of ivabradine on mouse (m) HCN1 and human (h) HCN4 channels heterologously expressed in HEK 293 cells. Ivabradine blocked both channels in a dose-dependent way with half-block concentrations of 0.94 μM for mHCN1 and 2.0 μM for hHCN4. Properties of block changed substantially for the two channels. Block of hHCN4 required open channels, was strengthened by depolarization and was relieved by hyperpolarization. Block of mHCN1 did not occur, nor was it relieved, when channels were in the open state during hyperpolarization; block required channels to be either closed, or in a transitional state between open and closed configurations. The dependence of block upon current flow was limited for hHCN4, and not significant for mHCN1 channels. In summary our results indicate that ivabradine is an 'open-channel' blocker of hHCN4, and a 'closed-channel' blocker of mHCN1 channels. The mode of action of ivabradine on the two channels is discussed by implementing a simplified version of a previously developed model of f-channel kinetics.

(Received 26 October 2005; accepted after revision 9 February 2006; first published online 16 February 2006)
Corresponding author D. DiFrancesco: Laboratory of Molecular Physiology and Neurobiology, Department of Biomolecular Sciences and Biotechnology, University of Milano, via Celoria 26, 20133 Milan, Italy.
Email: dario.difrancesco@unimi.it

The cardiac pacemaker (or 'funny', I_f) current is the main generator of the diastolic depolarization of cardiac sinoatrial node (SAN) cells, the phase of the action potential responsible for spontaneous, repetitive activity (DiFrancesco, 1993). Although described early in cardiac myocytes (Brown *et al.* 1979), its molecular building blocks were identified much later with the cloning, originally achieved by chance, of the hyperpolarization-activated cyclic nucleotide-gated (HCN) channel family in the late 1990s (Santoro *et al.* 1997, 1998; Gauss *et al.* 1998; Ludwig *et al.* 1998, 1999; Ishii *et al.* 1999; Seifert *et al.* 1999; Vaccari *et al.* 1999).

To date, this family includes four isoforms (HCN1–4), each one with distinct kinetic and modulatory properties and a specific distribution in a variety of tissues including cardiac and neuronal tissues (Accili *et al.* 2002; Robinson & Siegelbaum, 2003; Frere *et al.* 2004; Baruscotti *et al.* 2005). HCN channels belong to the superfamily of voltage-gated K^+ (Kv) and cyclic nucleotide-gated (CNG) channels. Their structure comprises six membrane-spanning (S1–6) domains which include a putative voltage sensor (S4) and a pore region between S5 and S6 carrying the GYG triplet signature of K^+-permeable channels, and a cyclic-nucleotide-binding domain (CNBD) in the C-terminus.

HCN isoforms are highly conserved in their core transmembrane regions and cyclic nucleotide binding domain (80–90% identical), but diverge in their amino- and carboxy-terminal cytoplasmic regions. When heterologously expressed, HCN channels display properties similar to those of native f/h-channels: permeability to Na^+ and K^+ ions, activation on hyperpolarization and modulation by cAMP, but their properties are quantitatively different (Accili *et al.* 2002).

Since HCN isoforms differ mostly in their N- and C-termini, these regions were investigated in the search

 DOI: 10.1113/jphysiol.2005.100776

for structural elements involved in isoform-specific kinetic and modulatory properties (Ulens & Tytgat, 2001; Viscomi *et al.* 2001; Wang *et al.* 2001; Xue *et al.* 2002; Ulens & Siegelbaum, 2003).

Isoform differences are the basis for the variability of native f/h-currents observed in different tissues. In several cases, however, the properties of native currents differ from those of any individual isoform, suggesting the contribution of several isoforms. Functional coassembly of heteromeric isoforms has been demonstrated both *in vitro* (Chen *et al.* 2001; Ulens & Tytgat, 2001; Altomare *et al.* 2003) and *in vivo* (Much *et al.* 2003) and may represent a mechanism able to provide a large range of functional variability to pacemaker f/h-channels.

This situation applies to sinoatrial f-channels, since their kinetics and modulatory properties do not match those described for any individual HCN isoforms; experiments based on mRNA and protein detection suggest that HCN4 is the major isoform, although contributions from HCN1 and HCN2 have also been determined (Shi *et al.* 1999; Moosmang *et al.* 2001; Moroni *et al.* 2001; Altomare *et al.* 2003).

Because of their relevance to the generation and control of pacemaker activity, f-channels have been the target for a pharmacological approach to heart rate regulation. The search for specific f-channel-blocking molecules is of special interest since these molecules have a potential for clinical use in cardiac dysfunctions where slowing of the heart rate is therapeutically beneficial, such as chronic angina and cardiac failure.

Several I_f-blocking drugs, such as alinidine (Snyders & Van Bogaert, 1987), cilobradine (Van Bogaert & Pittoors, 2003), zatebradine (Goethals *et al.* 1993; DiFrancesco, 1994), and ZD7288 (BoSmith *et al.* 1993), have been shown to act as bradycardic agents. More recently a compound with higher f-channel block specificity, ivabradine, has been developed (Thollon *et al.* 1994; Bois *et al.* 1996); ivabradine slows cardiac rate without complicating side-effects on action potential duration or inotropism; this specificity is a direct consequence of high selectivity of ivabradine for I_f (Bois *et al.* 1996).

In a previous investigation of the action of ivabradine in single rabbit SAN myocytes, we showed that ivabradine blocks I_f according to a complex mechanism (Bucchi *et al.* 2002). The drug is an open channel blocker, i.e. has free access to its binding site only when channels are in the open state, which requires hyperpolarization; at the same time, block develops preferentially when channels deactivate at depolarized voltages. These apparently contradictory features provide ivabradine with a strong 'use-dependence' of f-channel block, since efficient block is favoured by repetitive opening/closing cycles. Preferential block at depolarized voltages is a consequence of the fact that ivabradine molecules are positively charged and enter channel pores from their intracellular side. Indeed as a weak basic amine ($pK_a = 8.6$), ivabradine is largely in the protonated form at the extracellular pH of 7.4 (94.1%); the fraction in the neutral form (5.9%) equilibrates across the membrane and enters the cell, where the largest fraction (96.2%) is again ionized at the intracellular pH of 7.2.

However, experiments where the current flow through channels is varied independently of voltage (i.e. by means of channel block by external Cs^+ ions, or changes of external Na^+ concentration) show that the block is not voltage dependent *per se*, but is rather 'current' dependent. These data can be explained by assuming that ivabradine molecules interact with permeating ions in one of their binding sites in the pore, and reveal that permeation across f-channels is likely to occur according to a multi-ion, single-file process (Bucchi *et al.* 2002). In this respect the blocking mechanism operated by ivabradine differs markedly from that of other HCN channel blockers such as ULFS49 and ZD7288. For example, block of pacemaker channels by these latter drugs is not current dependent (Bucchi *et al.* 2002), despite both substances having, like ivabradine, a positively charged ammonium ion in their structure (BoSmith *et al.* 1993; Van Bogaert & Pittoors, 2003).

The experiments presented in this paper were devised to evaluate the action of ivabradine on two HCN subunits expressed in the SAN tissue, HCN1 and HCN4. Our data indicate that ivabradine exerts its block with different modalities for the two channels: while behaving as an 'open channel' blocker for HCN4, its behaviour with HCN1 channels is better described as that of a 'closed channel' blocker, since its interaction with HCN1 is allowed with closed states.

By incorporating these data in a simplified version of a previously developed model of HCN channel gating (Altomare *et al.* 2001), our results indicate that for both channels, drug binding is allowed not only when the channels are in open (HCN4) or closed (HCN1) states, but also when they are in transitional states available only when channels undergo repetitive stimulations.

Methods

Cell cultures and transfection

Human embryonic kidney cells (HEK 293, Phoenix) were cultured in Dulbecco's modified Eagle medium supplemented with 10% bovine calf serum (Invitrogen, Italy) and antibiotics (PenStrept from Sigma-Aldrich, Italy) at 37°C in 5% CO_2. hHCN4 or mHCN1 cDNA and the membrane antigen CD8 were cotransfected in HEK 293 cells with a standard calcium phosphate protocol. Four micrograms of either hHCN4 or mHCN1 cDNA and

2 μg of CD8 were used for each 35 mm Petri dish. Cells were used 2–3 days after transfection to allow for a good level of protein expression.

Electrophysiological recordings and data analysis

On the day of the experiments, transfected cells were dispersed by trypsin, plated at a low density on 35 mm plastic Petri dishes, and allowed to settle for 3–4 h. Prior to electrophysiological recordings, HEK 293 cells were incubated with Tyrode solution (mM: NaCl, 140; KCl, 5.4; $CaCl_2$, 1.8; $MgCl_2$, 1; D-glucose, 5.5; Hepes-NaOH, 5; pH 7.4) containing beads covered with antibodies (Dynabeads from Dynal Biotech ASA, Norway) specific for CD8 protein. Cell identification was obtained by placing Petri dishes on the stage of an inverted microscope; only cells presenting beads bound to the cell surface were selected for whole-cell patch-clamp analysis.

Cells were routinely perfused with a control Tyrode solution to which $BaCl_2$ (1 mM), $MnCl_2$ (2 mM), $NiCl_2$ (100 μM) and nifedipine (20 μM) were added to improve HCN current dissection. When necessary, ivabradine (3-(3-{[((7*S*)-3,4-dimethoxybicyclo[4,2,0]octa-1,3,5-trien-7-yl)methyl] methylamino}propyl)-1,3,4,5-tetrahydro-7,8-dimethoxy-2*H*-3-benzazepin-2-one, hydrochloride, from Institut de Recherches Internationales Servier, France; see Fig. 1*C*, right) was added to the extracellular solution by diluting a stock solution (0.1–20 mM) to the desired concentrations. Control and test solutions were delivered by a fast-perfusion temperature-controlled device allowing rapid (< 0.5 s) solution changes. Recording pipettes were filled with an intracellular-like solution containing (mM): potassium aspartate, 130; NaCl, 10; EGTA-KOH, 1; Hepes-KOH, 5; $MgCl_2$, 0.5; ATP (Na salt), 2; creatine phosphate, 5; GTP (Na salt), 0.1; pH 7.2. An Axopatch 200B amplifier and pCLAMP 7.0 software (Axon Instruments Inc., USA) were employed to record and on-line filter (corner frequency, 1 kHz) the HCN current traces. All experiments were carried out at the controlled temperature of 32 ± 1.0°C. Statistical analysis was performed using Student's one-sample and two-sample paired *t* tests; when comparing

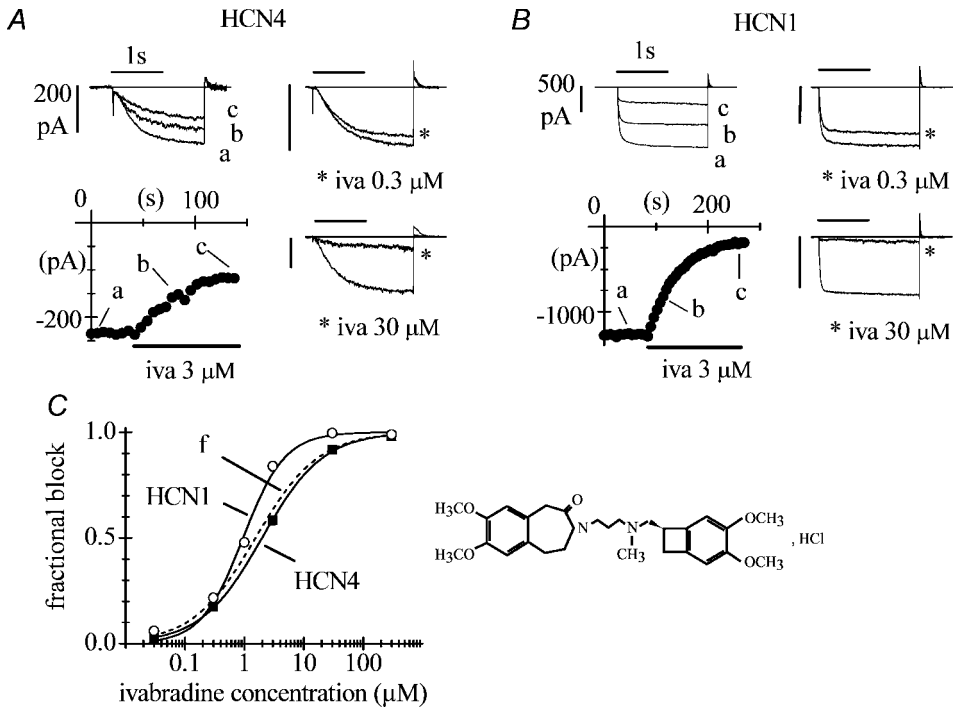

Figure 1. Block of HCN4 and HCN1 channels by ivabradine
A and *B*, pulsing protocol for block investigation: activating/deactivating steps (−100 mV, 1.8 s; +5 mV, 0.45 s) were applied every 6 s from a holding potential of −35 mV to cells expressing either HCN4 (*A*) or HCN1 channels (*B*), and ivabradine (iva) perfused until full block development. Typical time courses of I_{HCN4} and I_{HCN1} amplitudes at −100 mV are plotted during perfusion of 3 μM ivabradine (lower left panels in *A* and *B*). Sample current traces recorded just before (a) and during block development (b and c) for ivabradine 3 μM are plotted in upper left panels. Sample traces recorded in control and after full block (asterisks) also shown for 0.3 and 30 μM ivabradine in the right-hand panels in *A* and *B*. *C*, left, dose–response relationships of HCN4 (■, $n = 23$ cells) and HCN1 (○, $n = 27$ cells) channel block by ivabradine (mean ± S.E.M. (most error bars are smaller than symbol size)). Each cell was exposed to one drug dose only. Fitting data points with the Hill equation resulted in half-block concentrations of 2.0 and 0.94 μM and Hill factors of 0.8 and 1.2 for HCN4 and HCN1, respectively. *C*, right, ivabradine formula.

test *versus* control measurements, significance was set to $P < 0.05$.

Results

Ivabradine blocks HCN4 and HCN1 channels

Whole-cell HCN4 and HCN1 channel currents I_{HCN4} and I_{HCN1} were elicited by trains of activating/deactivating voltage steps (−100 mV, 1.8 s; +5 mV, 0.45 s) from a holding potential of −35 mV applied every 6 s (Fig. 1). When ivabradine was delivered onto the cell under study it caused a reduction of the current amplitude, which accumulated until steady-state block was reached. Figure 1 reports the time courses of I_{HCN4} and I_{HCN1} amplitudes at −100 mV during block onset in two representative experiments where cells were challenged with 3 μM drug concentration (lower left panels in Fig. 1*A* and *B*, respectively); sample traces, recorded at various times as indicated, are shown in upper left panels.

The mean steady-state current blocks caused by 3 μM ivabradine with this protocol were 58.2 ± 2.0% ($n = 5$) and 83.9 ± 2.0% ($n = 5$), and the mean time constants of block development (τ_{on}) were 48.1 ± 6.3 s ($n = 4$) and 61.2 ± 2.2 s ($n = 5$) for HCN4 and HCN1, respectively. Also shown in Fig. 1*A* and *B* are sample traces recorded in control and following full block by ivabradine at 0.3 and 30 μM (right-hand panels, as indicated).

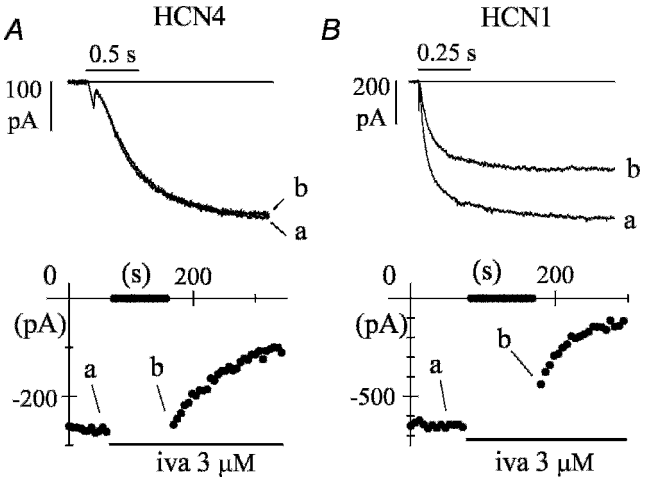

Figure 2. Block by ivabradine requires open HCN4, but does not require open HCN1 channels
A, time course of I_{HCN4} amplitude at −100 mV during a standard pulsing protocol (−100 mV, 1.8 s; +5 mV, 0.45 s). The cell was rested at −35 mV for the first 90 s of ivabradine (3 μM) perfusion before resuming the pulsing protocol. During the period at −35 mV no current reduction was observed. *B*, time course of I_{HCN1} amplitude at −100 mV during an identical protocol. In this case, during the time spent at −35 mV a significant current reduction was indeed observed, indicating partial block development. In *A* and *B*, sample traces recorded at various times as indicated.

Recovery from block was not investigated in these experiments; in pilot experiments we noticed that, as with ivabradine-induced block of native f-channels in SAN cells (Bucchi *et al.* 2002), the time constant of current recovery was slow and of the same order of magnitude as current run-down, which limited its correct evaluation.

Dose–response relations of mean I_{HCN4} and I_{HCN1} block obtained using the voltage protocol above for a range of drug concentrations are shown in Fig. 1*C*. Fitting the dose–response curves with the Hill equation yielded half-block concentrations of 2.0 μM and 0.94 μM and slope coefficients of 0.8 and 1.2 for HCN4 ($n = 23$) and HCN1 ($n = 27$) channels, respectively. The concentration-dependence of I_{HCN4} block, but not of I_{HCN1} block, was similar to that of the native I_f current in rabbit SAN cells (dashed line in Fig. 1*C*) reported previously (Bois *et al.* 1996; Bucchi *et al.* 2002). This is in agreement with evidence that HCN4 subunits represent the major contributors to native f-channels in the SAN (Shi *et al.* 1999; Ishii *et al.* 1999; Altomare *et al.* 2003; Stieber *et al.* 2003).

HCN4, but not HCN1 channels, need to be open for block to occur

To investigate if, as is the case with native f-channels, channel opening is a necessary requirement for ivabradine-induced block of either HCN4 or HCN1 to occur, activation/deactivation protocols (same as in Fig. 1) were applied. At the time of ivabradine (3 μM) application, the repetitive protocol was interrupted and the membrane held at −35 mV, a voltage at which HCN channels are closed; after 90 s in the continuous presence of ivabradine, the pulsing protocol was then resumed. The time courses of I_{HCN4} and I_{HCN1} amplitudes at −100 mV and sample current traces recorded before (a) and just after resuming the pulsing protocol (b, upper panels) are shown in Fig. 2 from two representative experiments.

Ivabradine did not show appreciable affinity for the closed conformation of HCN4 channels since no block developed while HCN4 channels were closed. As expected, resumption of activating/deactivating steps in the presence of the drug caused I_{HCN4} to decrease. In $n = 4$ cells, the mean ratio between the size of I_{HCN4} traces recorded at −100 mV just after and just before the 90 s pulsing protocol break was 0.98 ± 0.01 (not significantly different from 1). In contrast, application of the same protocol led to a reduction of I_{HCN1} even during the period spent at −35 mV (Fig. 2*B*), indicating that ivabradine could block HCN1 channels when they were closed. The mean ratio between currents at −100 mV measured just after and just before the 90 s interval was 0.87 ± 0.04 with 3 μM ivabradine ($n = 6$, see Fig. 3) and 0.93 ± 0.02 with 1 μM ivabradine ($n = 5$); both means were statistically

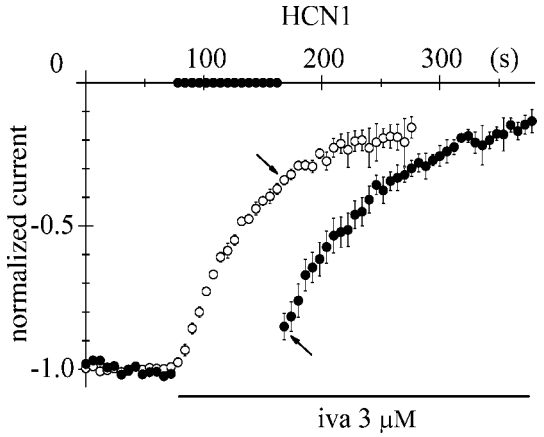

Figure 3. HCN1 block occurs preferentially when channels are cycling between open and closed states
Superimposition of the time course of block onset obtained with the protocol shown in Fig. 2*B* (●, mean ± S.E.M. of 6 cells) and the time course of block onset obtained with a standard activation/deactivation protocol (○, mean ± S.E.M. of 5 cells) after normalization of current amplitudes before block. The block developed during the 90 s period spent at −35 mV in the former case is less than that seen in the latter, when the pulsing protocol is not suspended (arrows), indicating that repetitive channel opening/closing cycles allow a more efficient block than having channels permanently closed.

different from 1. These results rule in favour of the hypothesis that for HCN1 channels, binding reaction and block occur in the closed state.

We next asked whether ivabradine could bind equally well to the open and closed states of HCN1 channels, or on the contrary could select among the two states. To investigate the relative affinity of open *versus* closed HCN1 states to ivabradine (3 μM), in Fig. 3 we superimposed the time courses of current at −100 mV during a standard activation/deactivation block protocol (open circles, mean of 5 cells) and during a pulse-interrupted protocol after normalization (filled circles, mean of 6 cells).

The superimposition shows that I_{HCN1} block occurs preferentially when channels are cycled between open and closed states. Indeed, comparison of the current amplitudes recorded 90 s after onset of drug perfusion (arrows) shows that the block generated during a standard activation/deactivation protocol, when channels were repeatedly open and closed, was much larger than that generated when channels were just kept closed during the interval at −35 mV. Thus, although the protocol of Fig. 3 does not allow the quantification of the relative ivabradine affinity ratio of open *versus* closed channels, it clearly indicates that repetitive opening of HCN1 channels favours the block reaction.

The results in Figs 1–3 show that drug molecules are able to access the binding sites of both HCN4 and HCN1 channels; for HCN4 channels, block occurs only when channels are open and therefore ivabradine behaves as an 'open channel' blocker, as found for native f-channels (Bucchi *et al.* 2002); on the other hand, HCN1 channels can be blocked in the closed configuration.

Steady-state block of I_{HCN4} and I_{HCN1} depends on the voltage protocol of current activation

Native I_f current block by ivabradine in SAN myocytes depends on the voltage protocol used to activate the current (Bucchi *et al.* 2002). We explored if the same applies to HCN4 and HCN1 currents by comparing the block induced by a standard activation/deactivation protocol with one where the current was activated with a single long hyperpolarizing step (Fig. 4).

Perfusion with 3 μM ivabradine during a standard activation/deactivation protocol caused a 60.9% inhibition of I_{HCN4} (Fig. 4*A*, left); with the same protocol, 1 μM ivabradine caused a 50.8% inhibition of I_{HCN1} in another experiment (Fig. 4*B*, left); these reductions were similar to

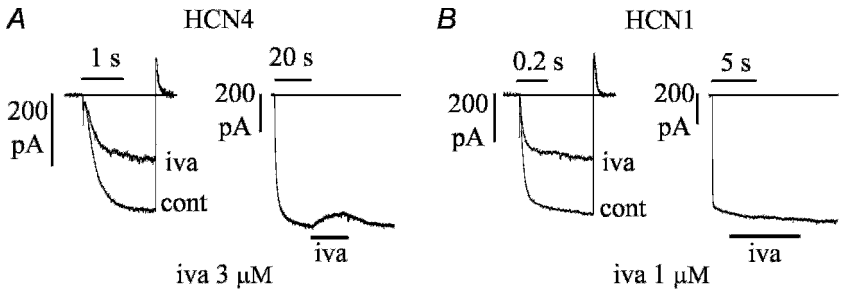

Figure 4. HCN4 and HCN1 currents are blocked by ivabradine according to the protocol used to activate them
A, left, I_{HCN4} records in control (cont) and after full block by 3 μM ivabradine induced by a standard activation/deactivation protocol at −100/+5 mV (as in Fig. 1); steady-state block was 60.9%. *A*, right, action of the same drug concentration when applied during steady-state I_{HCN4} activation at −100 mV; this protocol caused a block of 8.0%. *B*, similar experiments in an HCN1-expressing cell exposed to 1 μM ivabradine resulted in a 50.8% block of I_{HCN1} with the pulsing protocol (left) and in no blocking effect when the same drug concentration was applied during steady-state I_{HCN1} activation at −100 mV (right).

those previously obtained (Figs 1 and 2). In contrast, if the same drug concentrations were applied during long steps to −100 mV, after steady-state activation was reached, the block was much smaller for I_{HCN4} (8%, Fig. 4*A*, right) and undetectable for I_{HCN1} (Fig. 4*B*, right).

The mean I_{HCN4} block with the long-step protocol was 6.3 ± 0.8% at −100 mV ($n = 4$), a value much smaller than that obtained with activating/deactivating protocols (58.2 ± 2.0%, $n = 5$, as reported in Fig. 1). Even more surprising, we did not observe any measurable block of I_{HCN1} with 1 μM ivabradine ($n = 3$) during long-step current activation at −100 mV.

These large differences indicate that the drug–channel binding reaction and channel block are strongly affected by the voltage protocol used. If little or no block develops at hyperpolarized voltage levels, it means that most of the block observed with activating/deactivating protocols does not rely upon the channels being in the open configuration at steady state, but rather upon the repetitive cycling between open and closed states.

Although quantitative differences between HCN4 and HCN1 channels clearly exist, the data above indicate that for both channels, substantial block development requires repetitive opening/closing cycles.

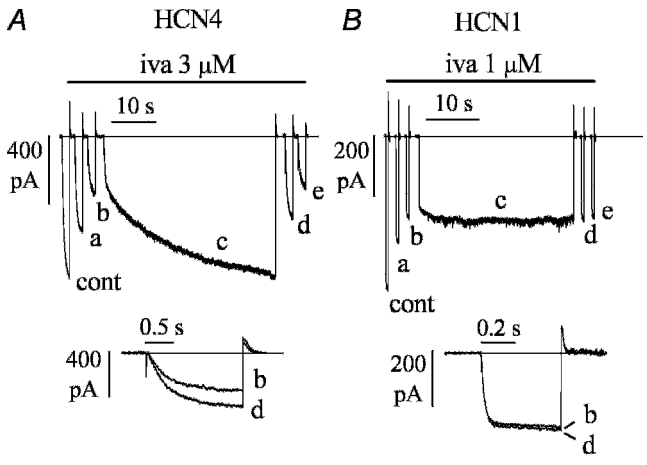

Figure 5. Block of HCN4, but not HCN1 channels, is reversed by hyperpolarization
A, I_{HCN4} block by 3 μM ivabradine was induced by a standard activation/deactivation protocol (−100 mV, 1.8 s; +5 mV, 1/6 Hz); records shown are: cont, control; a, 54 s, and b, 138 s after drug perfusion, the latter corresponding to steady-state block. In the continuous presence of the drug, a prolonged (40 s) step to −100 mV was then applied (trace c), following which the repetitive pulsing protocol resumed (traces d, 6 s, and e, 78 s after termination of the 40 s step). Superimposition of traces b and d (*A*, lower panel) shows that a partial block removal had occurred. *B*, in a similar experiment in an HCN1-expressing cell, a 30 s step to −100 mV was preceded and followed by standard pulsing protocols (−100 mV, 0.5 s; +5 mV, 1/6 Hz) during perfusion with ivabradine (1 μM); records shown are: cont, control; a, 138 s, and b, 258 s after drug perfusion (corresponding to steady-state block); d, 6 s, and e, 36 s after the 30 s long step. Superimposition of traces b and d (*B*, lower panel) shows that the current size did not change indicating the absence of block removal.

Hyperpolarization relieves ivabradine block of HCN4, but not of HCN1 channels

The results of Fig. 4 would be consistent with previous data in native f-channels indicating that ivabradine block development during activation/deactivation protocols results from an alternating process of block accumulation at depolarized voltages and block relief at hyperpolarized voltages (Bucchi *et al.* 2002). To verify if hyperpolarization-induced block relief is also observed with HCN4 and HCN1 isoforms, we used the analysis shown in Fig. 5.

In Fig. 5*A*, HCN4 block by 3 μM ivabradine was induced by a standard activation/deactivation protocol (−100/+5 mV); sample traces are shown (cont, before drug perfusion; a, 54 s, and b, 138 s after drug perfusion, the latter corresponding to steady-state block). In the continuous presence of the drug, a prolonged (40 s) step to −100 mV was then applied (c), at the end of which the repetitive pulsing protocol was re-applied (traces d and e, 6 and 78 s after step c, respectively). During the long step to −100 mV, a large fraction of HCN4 block was removed as apparent from the gradual current increase (trace c). A double-exponential fit of the current during the 40 s-long step revealed the presence of two kinetically different processes. While the early part of current activation developed with a time constant of 355.5 ms, a value similar to that of I_{HCN4} activation at −100 mV in control conditions (375.4 ms), the later increase developed with a much slower time constant (12.6 s), in agreement with the existence of two distinct processes. Based on its slow time course, the later current increase did not reflect channel activation kinetics, but possibly removal of block associated with unbinding of the drug.

The removal of block was most easily appreciated by superimposing traces d and b (Fig. 5*A*, lower panel), which clearly indicates that trace d, recorded just after the long pulse, was greater than trace b, recorded at steady-state block. Resuming the activation/deactivation protocol re-established block development (traces d and e).

In $n = 6$ cells, the mean time constants of current activation at −100 mV in control, in the early fraction of a > 25 s-long step to −100 mV during drug perfusion (3 μM), and on return from the long step to −100 mV were: 376.7 ± 29.4, 396.0 ± 36.0, and 389.8 ± 32.5 ms, respectively, while the slow increase at −100 mV had a time constant of 8.7 ± 1.9 s. These data indicate that ivabradine binds to HCN4 channels less favourably at hyperpolarized than at depolarized voltages.

A different behaviour was observed with HCN1 channels. In Fig. 5*B*, the same protocol as in Fig. 5*A* was applied to an HCN1-expressing cell during perfusion

with 1 μM ivabradine. In contrast to the result with HCN4, the long activating step (30 s) to −100 mV did not elicit a substantial current increase. Comparison of the records just before and just after the long step indeed indicated no significant change in I_{HCN1} amplitude at −100 mV (traces b and d). This protocol was repeated in six cells and the size of the current recorded after steady-state block by ivabradine (1 μM) was not substantially modified by applying a long (> 15 s) step to −100 mV (d/b = 1.03 ± 0.02, not significantly different from 1).

The interpretation of the results collected above therefore reveals different behaviours for the two isoforms: whereas in the case of HCN4, hyperpolarization relieves block, the HCN1 data show that at hyperpolarized voltages neither block nor block removal occur.

HCN4 block removal by hyperpolarization is favoured by inward current flow

Removal of ivabradine block of native f-channels during hyperpolarization is not due to voltage hyperpolarization *per se*, but rather to the inward ion flow, according to a 'current-dependent' blocking mechanism (Bucchi *et al.* 2002). We therefore wanted to verify if a similar mechanism also operates with HCN4 channels.

To test this hypothesis, we ran a long hyperpolarizing step protocol (as in Fig. 5) and verified the presence of block removal by hyperpolarization (Fig. 6, traces cont, a, b and c). Following resumption of the repetitive pulsing protocol (traces d and e), a second long (30 s) hyperpolarization to −100 mV was applied, during which Cs^+ (5 mM) was added to the perfusate in order to inhibit the inward ion flux through channels.

Cs^+ is a known extracellular blocker of f- and HCN channels whose action does not affect channel gating (DiFrancesco, 1982); in the presence of Cs^+, channels normally enter their open state on hyperpolarization, but no (or little) current is carried across the membrane (trace f). At the end of the long hyperpolarizing step, Cs^+ was washed out and the repetitive −100/+5 mV protocol was resumed (traces g and h). Superimposition of traces e and g (inset), recorded just before and just after the −100 mV step, shows that although a fraction of I_{HCN4} block was still removed, block removal was substantially smaller than in the absence of Cs^+. The mean ratios between the current amplitudes measured just after and just before the −100 mV step in the absence and in the presence of Cs^+ were 1.55 ± 0.09 and 1.30 ± 0.03 (n = 6), respectively. The mean ratios were statistically different according to t test and were both significantly different from 1. These results indicate that ivabradine block of HCN4 channels, like that of native f-channels, depends on the direction of current flow through channels. However, this dependence appears to be weaker than that found for f-channels, where inhibition of inward current flow by Cs^+ (5 mM) fully abolished hyperpolarization-induced block removal (Bucchi *et al.* 2002).

Voltage-dependence of ivabradine block of HCN4 and HCN1

To quantify the voltage-dependence of HCN4 block, we measured the steady-state current decrease caused by ivabradine (3 μM) at voltages ranging from −100 to +20 mV (Fig. 7*A*).

At voltages within the activation range (more negative than −40 mV), I_{HCN4} was activated by long steps to test potentials and, after steady-state activation had been reached, the drug was perfused until block fully developed (upper left panel in Fig. 7*A*). Fractional block was then measured as the ratio between blocked and control current amplitudes (open circles in Fig. 7*A*).

These data indicate that the fraction of blocked current decreased at more negative voltages and that at −100 mV the block was minimal (6.3 ± 0.8%, n = 4). We took advantage of this observation to measure the fractional block at voltages positive to the activation range

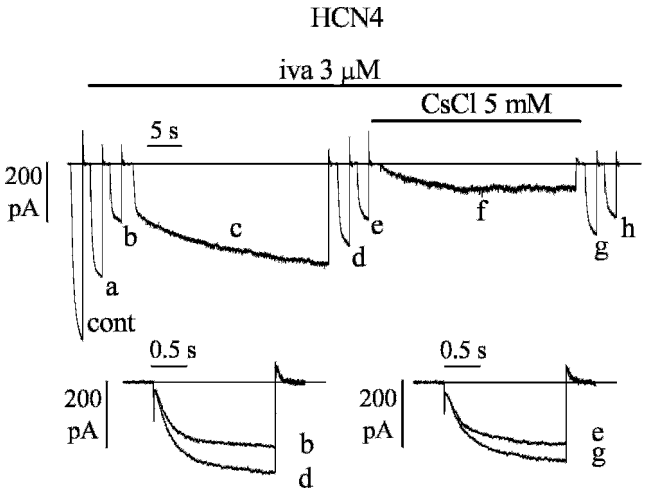

Figure 6. Inward current flow contributes to hyperpolarization-induced removal of HCN4 block by ivabradine
Block by 3 μM ivabradine was induced by a standard activation/deactivation protocol (−100/+5 mV); sample traces are shown on the left (cont, control; a, 54 s, and b, 150 s after drug application, the latter corresponding to steady-state block). A 30 s step to −100 mV was then applied in the continuous presence of the drug (trace c) and at the end of the 30 s step the repetitive pulsing protocol was resumed (traces d, 6 s, and e, 78 s after termination of the 30 s step). After reaching steady-state block for a second time (trace e), a new long (30 s) hyperpolarizing step to −100 mV was applied while simultaneously adding Cs^+ (5 mM); Cs^+ was washed off at the end of the new 30 s step and the repetitive pulsing protocol finally resumed (traces g, 6 s, and h, 60 s after Cs^+ wash-out). Lower panels: superimposition of traces b and d, and e and g indicate that block recovery was reduced in the presence of Cs^+.

(i.e. ≥ -50 mV). The cell membrane was held at a test potential in the range -50 to $+20$ mV and repetitive (1/6 Hz) steps to -100 mV for 1.2 s were applied (upper right panel in Fig. 7*A*); since at -100 mV little block occurs, and block removal requires long times (mean time constant of 8.7 ± 1.9 s, $n = 6$; see above), we can assume that the block obtained with this protocol develops almost entirely during current deactivation at the test voltage. Fractional block was thus measured for each test voltage as the ratio between blocked and control current at -100 mV at steady state (filled circles in Fig. 7*A*).

It should be noticed that at -50 mV both protocols were applied, and that the block values obtained did not coincide; indeed the block exerted by the drug during a long-step protocol was smaller than that observed with a pulsing protocol (0.19 ± 0.02, $n = 4$ *versus* 0.31 ± 0.02, $n = 3$). In addition, we observed that the fractional block at voltages equal to or more positive than -50 mV (pulsing protocol) showed a small sharp change across the reversal potential of the current (-21.3 ± 1.5 mV, $n = 5$; the block changed by 14% in the interval -30 to -20 mV), and then appeared to level out to a constant value of about 0.56 at depolarized voltages. This behaviour differs not only from that of a purely voltage-dependent block mechanism but also from that of a purely current-dependent block mechanism as found in native f-channels.

We next proceeded to study the voltage-dependence of steady-state HCN1 channel block by 1 μM ivabradine, using the same approach as for HCN4 (Fig. 7*B*). The two block protocols yielded two very different block values at -50 mV (0.03 ± 0.02, $n = 4$, open circles, *versus* 0.28 ± 0.03, $n = 5$, filled circles). The fractional block at voltages equal to or more positive than -50 mV (pulsing protocol) increased modestly with depolarization, and the change of block efficiency across the reversal potential of the current (-23.5 ± 1.7 mV, $n = 4$) was even smaller than for HCN4 (10% in the interval -30 to -20 mV); the block appeared to level out to a constant value of about 0.43 at the most depolarized voltages. At voltages equal to or more negative than -50 mV (long-step protocol), ivabradine had little if any blocking effect.

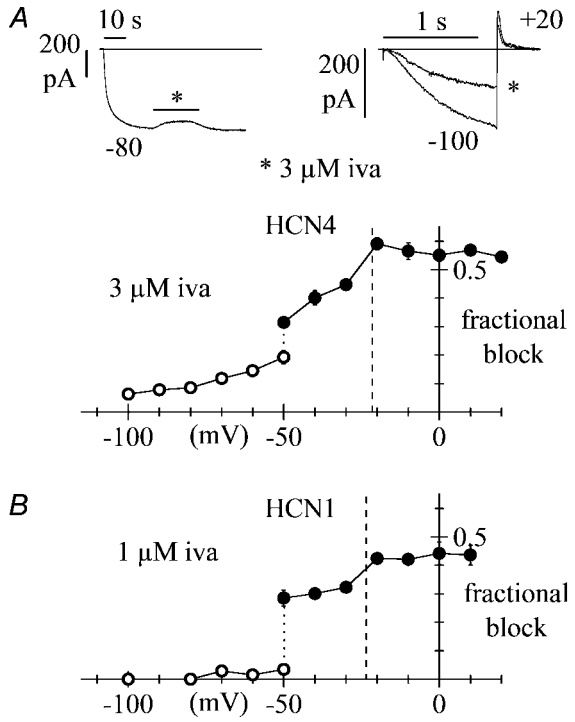

Figure 7. Voltage-dependence of steady-state block of HCN4 and HCN1 channels by ivabradine
Data are plotted as mean ± S.E.M. averaged from 3–13 cells (*A*, HCN4) or 3–5 cells (*B*, HCN1). For both curves, at voltages equal to or more negative than -50 mV the current was activated by long steps to test potentials and the drug perfused until full block development. Fractional block was measured as the ratio between blocked and control current amplitudes (○). At voltages equal to or more positive than -50 mV, the membrane was held at the test voltage and a fixed activating voltage step to -100 mV (*A*: 1.2 s; *B*: 0.5 s) was applied repetitively (1/6 Hz). Fractional block was then measured for each test voltage as the ratio between blocked and control current at -100 mV at steady-state (●). Vertical dotted lines correspond to the mean reversal potentials measured from fully activated current–voltage relations (HCN4: -21.3 ± 1.5 mV, $n = 5$; HCN1: -23.5 ± 1.7 mV; $n = 4$). Upper panels in *A* represent sample I_{HCN4} traces for the block protocols at -80 mV (left) and $+20$ mV (right: asterisk indicates current at steady-state block).

Proposed model of HCN4 and HCN1 block by ivabradine

The results of the action of ivabradine on HCN4 and HCN1 channels lead to a simple model that could account at least qualitatively for the experimental observations.

We have previously proposed a model in which the voltage-dependence of HCN channel gating was explained by an allosteric scheme (Altomare *et al.* 2001). This model assumed that HCN channels are tetramers, and that each subunit comprises a voltage sensor with two different configurations: a 'reluctant' one and a 'willing' one that favours the opening process. Whereas voltage sensors are independently gated by voltage, closed/open channel transitions occur allosterically and involve concerted structural modifications of all four subunits. This set of hypotheses leads to a multistate scheme comprising five open and five closed channel states. To describe the properties of HCN4 and HCN1 channel block by ivabradine, we have chosen here to adopt a simplified model where only states with all voltage sensors either in the reluctant or in the willing condition are considered. This reduces the Altomare *et al.* (2001) model to a 4-state scheme, as illustrated in Fig. 8.

Here, C and O states are characterized by all voltage sensors in the reluctant position, while C_4 and O_4 have all voltage sensors in the willing position. In

this context C_4 and O represent transitional states occupied by the channel only for brief periods during their normal activation/deactivation cycles between depolarized and hyperpolarized voltage levels. As in the previous model (Altomare *et al.* 2001), the present model assumes a voltage-dependence of rate constants favouring left-to-right and top-to-bottom transitions upon hyperpolarization. The activation process is therefore represented by first a 'priming' process, i.e. the displacement of the voltage sensors to their willing state ($C \rightarrow C_4$), and only subsequently by a distinct opening process ($C_4 \rightarrow O_4$). Similarly, deactivation is represented by first a change of the voltage sensors to their reluctant state ($O_4 \rightarrow O$), and then the proper channel closing process ($O \rightarrow C$). These sequences of events are obviously the most probable but not exclusive, since $C \rightarrow O \rightarrow O_4$ openings and $O_4 \rightarrow C_4 \rightarrow C$ closings are also possible, albeit with lower rates.

The action of ivabradine on HCN4 channels is described by assuming that the drug acts as a proper 'open channel' blocker and can therefore interact with open channel states only.

Interpretation of the HCN1 channel data, on the other hand, requires a different set of assumptions which lead to a selective affinity of free drug molecules for closed states only, as illustrated in the lower panel of Fig. 8.

The first assumption derives from the observation that open channels do not bind the free drug (Fig. 4*B*) and that block develops either during pulsing protocols or, at least partially, in the closed state (Figs 2, 3 and 4). The CB branch thus represents free drug binding at depolarized potentials in resting conditions (Fig. 2*B*), while the C_4B branch represents free drug binding during repetitive open/closed cycles (Figs 3 and 4*B*). Here we can further assume that the equilibrium of the binding reactions ($C + B \leftrightarrow CB$ and $C_4 + B \leftrightarrow C_4B$) favours the bound states (CB and C_4B), in agreement with the experimental evidence that recovery of the current is a slow process. It may be interesting to note that according to the model schemes proposed, repetitive cycling enhances HCN1 block during activation, when channels reach transiently state C_4, while HCN4 block is enhanced when channels pass through the transitional state O during deactivation.

A second assumption derives from the observation that after block development, no detectable unblocking occurs during long hyperpolarizing steps (Fig. 5*B*). This is taken into account by assuming the existence of open bound states OB and O_4B which will become populated at negative voltages but from which the drug cannot be released. Although these states are open, they are not conductive due to channel block. Note that according to the scheme, open–bound states can only be formed starting from closed–bound states and are not connected to the open states O and O_4, to account for the lack of free drug binding to/unbinding from open states; this is consistent with the view that drug molecules may be 'trapped' in the open channel configuration and require channel closing to be released.

The model schemes of Fig. 8 also allow an interpretation of the differences in block values observed in Fig. 7 at −50 mV by the use of two different measuring protocols, i.e. long-step protocol (open circles) and the pulsing protocol (filled circles). Considering for example the HCN1 scheme (Fig. 8*B*), with the first protocol the measured block represents the fraction of channels in the O_4 state which will become blocked at −50 mV at steady state, which according to the model is nil. With the second protocol, the voltage is stepped repetitively between −50 and −100 mV, and occupancies will be significant for all the four states (C, C_4, O_4, O); clearly under these conditions, the fraction of open channels blocked at steady state will also be significant (Fig. 7*B*). Similar considerations apply to HCN4 (−50 mV point in Fig. 7*A*). In this case, while the long step protocol again measures the block fraction for state O_4, the pulsing protocol measures in addition that for state O. The difference between the two block values is smaller than for HCN1, reflecting a substantial blocking efficiency for state O_4 of HCN4 channels.

Possible reasons for preferential binding of the drug to certain channel configurations probably involve specific interactions of the drug molecule with channel residues aligning the channel pore and undergoing spatial rearrangement during changes of channel state.

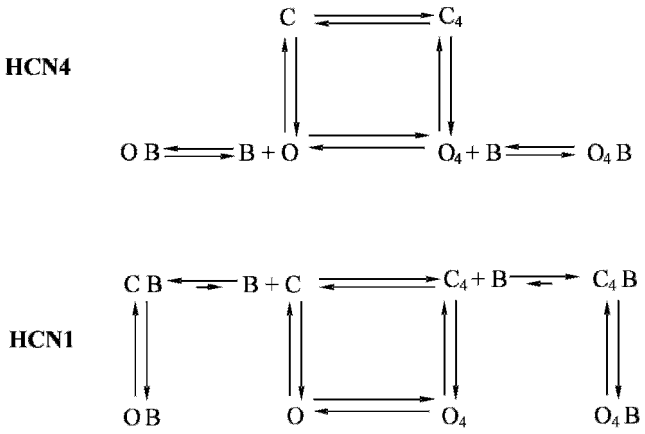

Figure 8. Model scheme for ivabradine binding to HCN4 and HCN1 channels
The scheme is a simplification of the Altomare *et al.* (2001) model considering only channel states where voltage sensors are all in either the reluctant (C, O) or the willing state (C_4, O_4). C indicates closed channels, O open channels and B blocking molecules. Upper panel: block of HCN4. In this case the drug operates as an 'open' channel blocker and only interferes with open channel states. Lower panel: block of HCN1. Here free drug molecules can bind to closed, but not to open states. Further explanation in text.

Discussion

'Funny' (f-) channels play a key role in the generation of spontaneous activity of pacemaker cells, and mediate autonomic control of cardiac rate. Pharmacological agents able to interfere with their function can therefore be exploited in principle for a selective control of cardiac rhythm. Ivabradine, a heart rate-reducing agent, is able to lower heart rate by blocking f-channels of the pacemaker region of the heart. Since ivabradine displays a high selectivity for f-channels, its action lacks significant side-effects (such as for example a decrease of cardiac inotropism) typical of less specific blockers which also interfere which other channels (Satoh & Hashimoto, 1986; Goethals *et al.* 1993; Thollon *et al.* 1994; Perez *et al.* 1995).

Evidence from mRNA and protein distribution, along with the kinetic and modulatory properties of native f/h-channels studied in various tissues (for example thalamus, hippocampus, SAN, ventricles), clearly indicates that native channels may result from the heterologous assembly of different isoforms (Chen *et al.* 2001; Ulens & Tytgat, 2001; Altomare *et al.* 2003). In the rabbit SAN, HCN4 is the major subunit contributing to the native f-channel structure, although limited yet functionally relevant amounts of HCN1 (and possibly HCN2) have also been reported (Shi *et al.* 1999; Moroni *et al.* 2001). It is therefore appropriate that any drug acting on native currents is dually characterized, firstly to assess the blocking properties on the native current itself, and secondly to evaluate the action of the drug on individual HCN isoforms likely to contribute to the native channels. Indeed differences of action on different isoforms can provide useful information and help design future molecules with isoform-specific, and thus possibly tissue-specific selectivity.

In the present study, we provide a specific characterization of the blocking effect of ivabradine on the two HCN proteins known to be expressed in rabbit SAN tissue, HCN4 and HCN1. The effect of the drug was first tested with repetitive trains of activation/deactivation steps (−100/+5 mV, as in Fig. 1). With this protocol, channels loop between open and closed states and, when channels are open, the current flow can be either inward (−100 mV) or outward (+5 mV). The time courses of I_{HCN4} and I_{HCN1} block induced by ivabradine with the pulsing protocol indicate the presence of block accumulation which develops with time constants of the order of several tens of seconds (Fig. 1). Dose–response analysis revealed that the dose–response relationships of ivabradine block of HCN4 and of native f-channels (Bucchi *et al.* 2002) are nearly overlapping (Fig. 1*C*). From Hill fitting, the half-block concentrations were 2.0 and 1.5 μM for HCN4 and native channels, respectively, and the Hill slope was 0.8 in both cases. The dose–response relationship of HCN1 block, on the other hand, differed more markedly from that of f-channels (half-block concentration of 0.94 μM and Hill slope of 1.2, Fig. 1*C*). A higher Hill slope for the HCN1 curve might imply a higher degree of co-operativity in drug binding to HCN1 relative to HCN4 and native f-channels.

Ivabradine is an 'open' HCN4 channel blocker

Analysis of the dependence of drug binding on the channel state was investigated with the experiments of Fig. 2. In those experiments, we tried to establish whether the drug binds HCN4 or HCN1 channels with a preferential affinity for the closed or open configurations. In agreement with the results obtained in native channels, the I_{HCN4} block occurred only when HCN4 channels were open (Fig. 2*A*) indicating that the binding site is not accessible in the closed state. Surprisingly, results obtained with HCN1 revealed that ivabradine reaches its site of action also when channels are closed, although less easily than when they are cycled between open and closed states (Figs 2*B* and 3). In relation to these results, it is important to note that when compared to HCN1, HCN4 channels have bulkier N- and C- termini located in the cytoplasmic region below the channel mouth, and that these structures could participate in limiting the drug access to the channel binding site.

A most remarkable property of ivabradine blockade of native f-channels is its current-dependence. We have previously demonstrated that ivabradine action on I_f depends strongly upon the direction of current flow. Indeed, a sudden change of block value was measured across the current reversal potential (Fig. 7 of Bucchi *et al.* 2002). Our results with HCN4 channel block also indicate the presence of a dependence on the direction of current flow, although this is less marked than for native f-channels.

Evidence for a partial current-dependence of block comes, for example, from the Cs^+ experiment of Fig. 6, since Cs^+-induced HCN4 inhibition should not reduce the hyperpolarization-driven removal of block if this simply depended on voltage.

Analysis of the voltage-dependence of block (Fig. 7*A*) provides further evidence for the hypothesis that hyperpolarization-induced removal of HCN4 block by ivabradine has both a 'voltage-dependent' and a 'current-dependent' component. The plot of Fig. 7*A* shows that at voltages where the current is outward, a steady-state level of block is reached and the block–voltage relation flattens (as is observed with f-channels). Moving towards more negative voltages, the block curve undergoes a sudden change when crossing the reversal potential of I_{HCN4} (between −20 and −30 mV), indicating a 'current-dependent' component; however, this change is much less dramatic than that observed with f-channels (compare with Fig. 7 of Bucchi *et al.* 2002); a substantial

'voltage-dependent' component of block which is not attributable to current reversal is evident in the range negative to −30 mV. Thus, the direction of current flow can only account for part of the voltage-dependence of ivabradine block of HCN4 channels.

Ivabradine is a 'closed' HCN1 channel blocker

The results obtained with HCN1 channels differ in several aspects from those of HCN4 and native rabbit f-channels. Indeed, experiments such as those in Figs 4*B* and 7*B* clearly demonstrate that the drug has little or no effect when channels are kept open. The lack of effect at hyperpolarized voltages is confirmed by experiments such as those of Fig. 5*B* where hyperpolarization is unable to induce the removal of a previously induced block.

From these observations we conclude that binding/unbinding of ivabradine to HCN1 channels is not allowed when channels are open, and that the I_{HCN1} current flow does not affect the drug–channel interaction. However, while on the one hand the results of Figs 4*B* and 5*B* indicate no affinity of the drug for the open state, the results of Fig. 3 show that repetitive stepping between open and closed states is a more favourable condition for block to occur than when channels are permanently kept in the closed state.

This led us to consider the hypothesis, proposed in the model scheme of Fig. 8, that ivabradine might bind preferentially to HCN1 channels when they are in a transitional state between closed and open configurations. This hypothesis is compatible with the observation that when steady-state block is evaluated at −50 mV by a stepping procedure (filled circle at −50 mV in Fig. 7*B*), the repetitive switching between closed and open states favours block development relative to the protocol when block is evaluated during a long step to −50 mV (open circle at −50 mV in Fig. 7*B*).

Limitations of the study

A limitation of this study concerns the species difference between channel isoforms (human HCN4 *versus* mouse HCN1). Although the qualitative differences in properties of drug block of the two isoforms are unlikely to be species dependent, quantitative features of block might be. Because of the therapeutical use of ivabradine (Baruscotti *et al.* 2005), it will be interesting to investigate the details of drug block of the human HCN1 isoform.

Conclusions

Our data show that the mechanisms of ivabradine block of the two HCN channel isoforms HCN1 and HCN4 differ substantially as illustrated by the reaction schemes of Fig. 8. This is indicated by several different aspects of HCN1 and HCN4 block, including the concentration-dependence, suggesting unequal co-operativities, and the dependence upon voltage (Fig. 7). An even more striking difference relates to the state-dependence of channel block: while HCN4 block, as in native f-channels, has the properties of an open-channel block, that of HCN1 is a closed channel block. Clearly, therefore, binding of the drug to channels will depend crucially upon the interaction with specific residues likely to be different, or spatially orientated in a different way, in the two channel isoforms. A more detailed analysis will therefore require site-specific mutagenesis to identify the actual residues involved in drug binding.

References

Accili EA, Proenza C, Baruscotti M & DiFrancesco D (2002). From funny current to HCN channels: 20 years of excitation. *News Physiol Sci* **17**, 32–37.

Altomare C, Bucchi A, Camatini E, Baruscotti M, Viscomi C, Moroni A & DiFrancesco D (2001). Integrated allosteric model of voltage gating of HCN channels. *J Gen Physiol* **117**, 519–532.

Altomare C, Terragni B, Brioschi C, Milanesi R, Pagliuca C, Viscomi C, Moroni A, Baruscotti M & DiFrancesco D (2003). Heteromeric HCN1-HCN4 channels: a comparison with native pacemaker channels from the rabbit sinoatrial node. *J Physiol* **549**, 347–359.

Baruscotti M, Bucchi A & DiFrancesco D (2005). Physiology and pharmacology of the cardiac pacemaker ('funny') current. *Pharmacol Ther* **107**, 59–79.

Bois P, Bescond J, Renaudon B & Lenfant J (1996). Mode of action of bradycardic agent, S 16257, on ionic currents of rabbit sinoatrial node cells. *Br J Pharmacol* **118**, 1051–1057.

BoSmith RE, Briggs I & Sturgess NC (1993). Inhibitory actions of ZENECA ZD7288 on whole-cell hyperpolarization activated inward current (If) in guinea-pig dissociated sinoatrial node cells. *Br J Pharmacol* **110**, 343–349.

Brown HF, DiFrancesco D & Noble SJ (1979). How does adrenaline accelerate the heart? *Nature* **280**, 235–236.

Bucchi A, Baruscotti M & DiFrancesco D (2002). Current-dependent block of rabbit sino-atrial node If channels by ivabradine. *J Gen Physiol* **120**, 1–13.

Chen S, Wang J & Siegelbaum SA (2001). Properties of hyperpolarization-activated pacemaker current defined by coassembly of HCN1 and HCN2 subunits and basal modulation by cyclic nucleotide. *J Gen Physiol* **117**, 491–504.

DiFrancesco D (1982). Block and activation of the pace-maker channel in calf Purkinje fibres: effects of potassium, caesium and rubidium. *J Physiol* **329**, 485–507.

DiFrancesco D (1993). Pacemaker mechanisms in cardiac tissue. *Annu Rev Physiol* **55**, 455–472.

DiFrancesco D (1994). Some properties of the UL-FS 49 block of the hyperpolarization-activated current (I_f) in sino-atrial node myocytes. *Pflugers Arch* **427**, 64–70.

Frere SG, Kuisle M & Luthi A (2004). Regulation of recombinant and native hyperpolarization-activated cation channels. *Mol Neurobiol* **30**, 279–305.

Gauss R, Seifert R & Kaupp UB (1998). Molecular identification of a hyperpolarization-activated channel in sea urchin sperm. *Nature* **393**, 583–587.

Goethals M, Raes A & van Bogaert P-P (1993). Use-dependent block of the pacemaker current I_f in rabbit sinoatrial node cells by zatebradine (UL-FS 49): On the mode of action of sinus node inhibitors. *Circulation* **88**, 2389–2401.

Ishii TM, Takano M, Xie LH, Noma A & Ohmori H (1999). Molecular characterization of the hyperpolarization-activated cation channel in rabbit heart sinoatrial node. *J Biol Chem* **274**, 12835–12839.

Ludwig A, Zong X, Jeglitsch M, Hofmann F & Biel M (1998). A family of hyperpolarization-activated mammalian cation channels. *Nature* **393**, 587–591.

Ludwig A, Zong X, Stieber J, Hullin R, Hofmann F & Biel M (1999). Two pacemaker channels from human heart with profoundly different activation kinetics. *EMBO J* **18**, 2323–2329.

Moosmang S, Stieber J, Zong X, Biel M, Hofmann F & Ludwig A (2001). Cellular expression and functional characterization of four hyperpolarization-activated pacemaker channels in cardiac and neuronal tissues. *Eur J Biochem* **268**, 1646–1652.

Moroni A, Gorza L, Beltrame M, Gravante B, Vaccari T, Bianchi ME, Altomare C, Longhi R, Heurteaux C, Vitadello M, Malgaroli A & DiFrancesco D (2001). Hyperpolarization-activated cyclic nucleotide-gated channel 1 is a molecular determinant of the cardiac pacemaker current I_f. *J Biol Chem* **276**, 29233–29241.

Much B, Wahl-Schott C, Zong X, Schneider A, Baumann L, Moosmang S, Ludwig A & Biel M (2003). Role of subunit heteromerization and N-linked glycosylation in the formation of functional hyperpolarization-activated cyclic nucleotide-gated channels. *J Biol Chem* **278**, 43781–43786.

Perez O, Gay P, Franqueza L, Carron R, Valenzuela C, Delpon E & Tamargo J (1995). Effects of the two enantiomers, S-16257-2 and S-16260-2, of a new bradycardic agent on guinea-pig isolated cardiac preparations. *Br J Pharmacol* **115**, 787–794.

Robinson RB & Siegelbaum SA (2003). Hyperpolarization-activated cation currents: from molecules to physiological function. *Annu Rev Physiol* **65**, 453–480.

Santoro B, Grant SGN, Bartsch D & Kandel ER (1997). Interactive cloning with the SH3 domain of N-src identifies a new brain specific ion channel protein, with homology to Eag and cyclic nucleotide- gated channels. *Proc Natl Acad Sci U S A* **94**, 14815–14820.

Santoro B, Liu DT, Yao H, Bartsch D, Kandel ER, Slegelbaum SA & Tibbs GR (1998). Identification of a gene encoding a hyperpolarization-activated pacemaker channel of brain. *Cell* **93**, 717–729.

Satoh H & Hashimoto K (1986). Electrophysiological study of alinidine in voltage clamped rabbit sino-atrial node cells. *Eur J Pharmacol* **121**, 211–219.

Seifert R, Scholten A, Gauss R, Mincheva A, Lichter P & Kaupp UB (1999). Molecular characterization of a slowly gating human hyperpolarization-activated channel predominantly expressed in thalamus, heart, and testis. *Proc Natl Acad Sci U S A* **96**, 9391–9396.

Shi W, Wymore R, Yu H, Wu J, Wymore RT, Pan Z, Robinson RB, Dixon JE, McKinnon D & Cohen IS (1999). Distribution and prevalence of hyperpolarization-activated cation channel (HCN) mRNA expression in cardiac tissues. *Circ Res* **85**, e1–e6.

Snyders DJ & Van Bogaert P-P (1987). Alinidine modifies the pacemaker current in sheep Purkinje fibers. *Pflugers Arch* **410**, 83–91.

Stieber J, Herrmann S, Feil S, Loster J, Feil R, Biel M, Hofmann F & Ludwig A (2003). The hyperpolarization-activated channel HCN4 is required for the generation of pacemaker action potentials in the embryonic heart. *Proc Natl Acad Sci U S A* **100**, 15235–15240.

Thollon C, Cambarrat C, Vian J, Prost J-F, Peglion JL & Vilaine JP (1994). Electrophysiological effects of S 16257 a novel sino-atrial node modulator, on rabbit and guinea-pig cardiac preparations: Comparison with UL-FS 49. *Br J Pharmacol* **112**, 37–42.

Ulens C & Siegelbaum SA (2003). Regulation of hyperpolarization-activated HCN channels by cAMP through a gating switch in binding domain symmetry. *Neuron* **40**, 959–970.

Ulens C & Tytgat J (2001). Functional heteromerization of HCN1 and HCN2 pacemaker channels. *J Biol Chem* **276**, 6069–6072.

Vaccari T, Moroni A, Rocchi M, Gorza L, Bianchi ME, Beltrame M & DiFrancesco D (1999). The human gene coding for HCN2, a pacemaker channel of the heart. *Biochim Biophys Acta* **1446**, 419–425.

Van Bogaert PP & Pittoors F (2003). Use-dependent blockade of cardiac pacemaker current (If) by cilobradine and zatebradine. *Eur J Pharmacol* **478**, 161–171.

Viscomi C, Altomare C, Bucchi A, Camatini E, Baruscotti M, Moroni A & DiFrancesco D (2001). C terminus-mediated control of voltage and cAMP gating of hyperpolarization-activated cyclic nucleotide-gated channels. *J Biol Chem* **276**, 29930–29934.

Wang J, Chen S & Siegelbaum SA (2001). Regulation of hyperpolarization-activated HCN channel gating and cAMP modulation due to interactions of COOH terminus and core transmembrane regions. *J Gen Physiol* **118**, 237–250.

Xue T, Marban E & Li RA (2002). Dominant-negative suppression of HCN1- and HCN2-encoded pacemaker currents by an engineered HCN1 construct: insights into structure-function relationships and multimerization. *Circ Res* **90**, 1267–1273.

Acknowledgements

We would like to thank the Institut de Recherches Internationales Servier for providing support for this work. This work was partially supported by FIRB 2001 and PRIN 2003 grants to D.D.